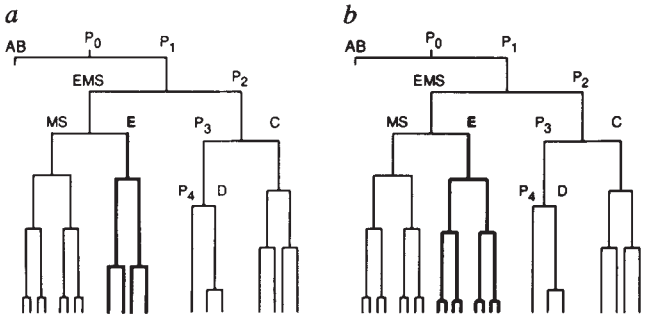

FIG. 4 *a*, Partial lineage of intact embryo. *b*, Partial lineage of embryos in which P_2 and EMS were separated and gut did not differentiate, showing the relative order of division of cells. The E lineage takes on MS-like cleavage times when the induction is blocked. (9/9 cases observed, from the 19 that did not differentiate gut, shown in Fig. 3*a*.)

the AB lineage[4,8,9]. No other lineages were previously known to require cell interactions during early development.

Two pieces of information raise the possibility that many other inductions may be occurring during early *C. elegans* development. First, this work shows that previous methods could not detect all cell interactions. Second, most issues in *C. elegans* arise from many distantly related cells, not from the progeny of a single founder cell[2] (Fig. 1*b*); segregation of determinants would have to be extraordinarily complex to generate this sort of lineage independently of inductions, considering that determinants for at least several cell types are not prelocalized in the egg[10].

Given the organism's amenability to genetic analysis, the finding that gut is induced and the possibility that many other inductions may be occurring in *C. elegans* may afford us a chance to understand the molecular mechanisms that underlie embryonic inductions. □

Received 7 November 1991; accepted 7 April 1992.

1. Davidson, E. H. *Gene Activity in Early Development* 3rd edn (Academic, Orlando, 1986).
2. Sulston, J. E. *et al. Devl Biol.* **100,** 64–119 (1983).
3. Schierenberg, E. *Devl Biol.* **122,** 452–463 (1987).
4. Priess, J. R. & Thomson, J. N. *Cell* **48,** 241–250 (1987).
5. Laufer, J. S. *et al. Cell* **19,** 569–577 (1980).
6. Edgar, L. G. & McGhee, J. D. *Devl Biol.* **114,** 109–118 (1986).
7. Maine, E. M. & Kimble, J. *BioEssays* **12,** 265–271 (1990).
8. Wood, W. B. *Nature* **349,** 536–538 (1991).
9. Schnabel, R. *Mech. Dev.* **34,** 85–100 (1991).
10. Laufer, J. S. & von Ehrenstein, G. *Science* **211,** 402–405 (1981).
11. Sulston, J. & Hodgkin, J. in *The Nematode* Caenorhabditis elegans (ed. Wood, W. B.) 587–606 (Cold Spring Harbor Laboratory Press, New York, 1988).
12. Chitwood, B. G. & Chitwood, M. B. *Introduction to Nematology* (University Park, Baltimore, 1974).

ACKNOWLEDGEMENTS. I thank G. Freeman for advice, C. Jenkins, G. Freeman and others for critically reading the manuscript, and L. Edgar for protocols for isolating and culturing blastomeres. Worms were provided by D. Barker and by the *Caenorhabditis* Genetics Center, which is funded by the NIH National Center for Research Resources. This work was supported by an NSF grant to Gary Freeman and an NIH predoctoral training grant to the author.

The rate of actin-based motility of intracellular *Listeria monocytogenes* equals the rate of actin polymerization

Julie A. Theriot*, Timothy J. Mitchison†, Lewis G. Tilney‡ & Daniel A. Portnoy§

Departments of * Biochemistry and Biophysics and † Pharmacology, University of California, San Francisco, California 94143, USA
‡ Department of Biology, University of Pennsylvania and
§ Department of Microbiology, University of Pennsylvania School of Medicine, Philadelphia, Pennsylvania 19104, USA

THE Gram-positive bacterium *Listeria monocytogenes* is a facultative intracellular pathogen capable of rapid movement through the host cell cytoplasm[1]. The biophysical basis of the motility of *L. monocytogenes* is an interesting question in its own right, the answer to which may shed light on the general processes of actin-based motility in cells. Moving intracellular bacteria display phase-dense 'comet tails' made of actin filaments, the formation of which is required for bacterial motility[2,3]. We have investigated the dynamics of the actin filaments in the comet tails using the technique of photoactivation of fluorescence, which allows monitoring of the movement and turnover of labelled actin filaments after activation by illumination with ultraviolet light. We find that the actin filaments remain stationary in the cytoplasm as the bacterium moves forward, and that length of the comet tails is linearly proportional to the rate of movement. Our results imply that the motile mechanism involves continuous polymerization and release of actin filaments at the bacterial surface and that the rate of filament generation is related to the rate of movement. We suggest that actin polymerization provides the driving force for bacterial propulsion.

L. monocytogenes can move in many cell types, and we chose to infect the flat and easily injectible potoroo kidney epithelial (PtK2) cell line. As reported[1], *L. monocytogenes* induced the formation of actin-filament-rich phase-dense comet tails and moved at rates of up to 0.4 μm per second through the cytoplasm of these cells. The tails appear substantially shorter by phase contrast than by rhodamine–phalloidin labelling, which marks filamentous actin (Fig. 1*a*, *b*). Fluorescence intensity profiles of phalloidin-labelled tails reveal that there is a pronounced gradient of actin filament density through the tail, such that the filament density is highest closest to the bacterium and decreases exponentially towards the distal top (Fig. 1*c*). The tail is visible by phase microscopy as long as 30–50% of the peak density of actin filaments in the tail persist.

To probe *L. monocytogenes* tail actin filament dynamics, infected cells were microinjected with purified rabbit skeletal muscle G-actin covalently coupled to caged resorufin (CR)[4]. CR-actin is nonfluorescent and readily incorporates into endogenous actin structures in microinjected cells, including stress fibres and lamellipodia. Upon illumination with ultraviolet light at 360 nm, CR is rapidly and efficiently converted to the bright red fluorescent parent compound, resorufin. The movement and turnover of activated labelled actin filaments can then be followed by fluorescence videomicroscopy[4]. Short segments of the actin tails of moving *L. monocytogenes* were photoactivated[5]. The marked filaments were imaged by fluorescence and the moving bacteria by phase-contrast; the two images were superimposed electronically. We marked the tails of 22 bacteria moving at rates ranging from 0.02 to 0.20 μm per second. In each case, the photoactivated mark on the tail remained stationary in the cytoplasm as the bacterium moved away from the mark (Fig. 2). Movement or splitting of the activated region was never observed; given the limits of sensitivity of this technique, at least 95% of the actin filaments in the tail are stationary in the cytoplasm as the bacterium moves. We conclude that filaments must appear continuously at the bacterium surface, and be released from the bacterium as it moves on, so the rate of bacterium movement is simply equal to the rate of actin filament appearance.

To investigate the stability of tail actin filaments, we measured the decay in intensity of the fluorescent mark under conditions of negligible photobleaching. Fluorescence decay was exponential, and the average turnover rate was 33 s (s.d. = 16, $n = 22$). By comparison, the average half-life of actin filaments in stress fibres in PtK2 cells is 230 s (ref. 4). There was no correlation between filament half-life and rate of bacterium movement

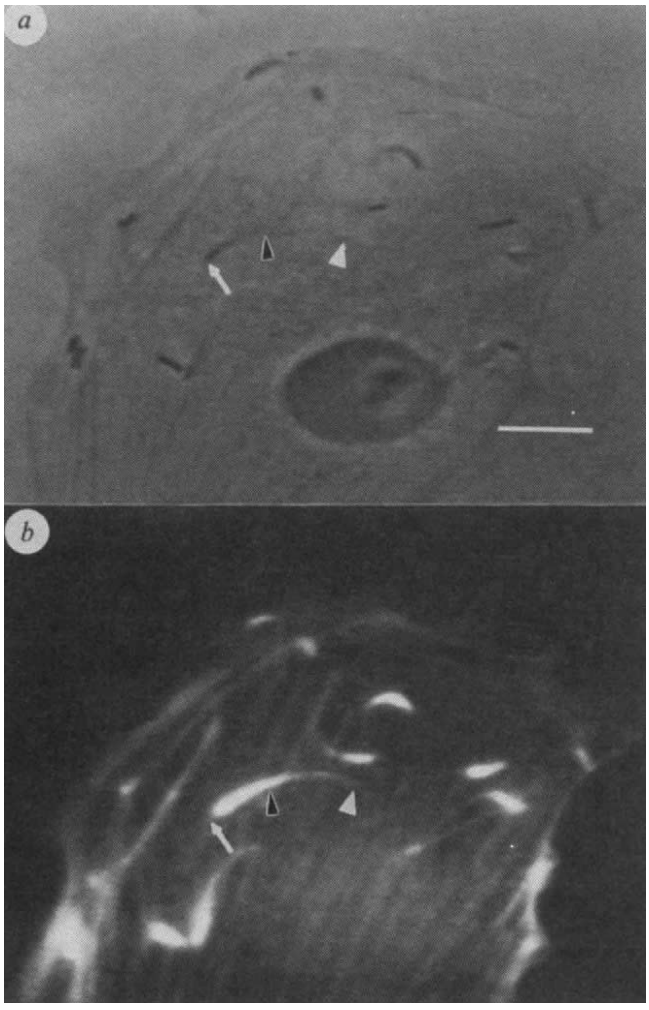

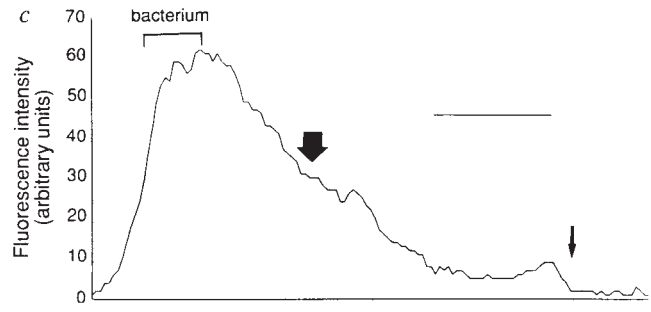

FIG. 1 Actin filament organization in *L. monocytogenes* tails. *a*, Phase and *b*, fluorescence images of a single infected cell fixed and labelled with rhodamine-phalloidin. White arrows indicate the position of the front of the bacterium, black arrowheads indicate the end of the tail visible by phase, and white arrowheads indicate the end of the tail visible by fluorescence. Note that the tails are substantially longer when visualized with fluorescent phalloidin. Scale bar, 10 μm. *c*, Fluorescence intensity profile of a single *L. monocytogenes* tail labelled with rhodamine-phalloidin. The thick arrow marks the end of the tail visible by phase microscopy and the thin arrow the end of the tail visible by fluorescence. The shape of the intensity profile approximates exponential decay. This example is representative of 12 tails examined. The peak of actin filament density is slightly behind the bacterium, which is consistent with the distribution of actin filaments seen by electron microscopy[2,3]. Scale bar, 5 μm.

METHODS. PtK2 cells were grown as described[5] on acid-washed glass coverslips and infected[1] with *L. monocytogenes* strain 10403S. Three hours after infection, a coverslip was transferred to a heated aluminium chamber and motility was observed using phase-contrast videomicroscopy. Cells were fixed *in situ* by replacing the medium with 3.2% formaldehyde in PBS, and actin filaments were labelled with 1 μg ml^{-1} rhodamine-phalloidin. The appearance and length of the tails visible by phase were identical before and after fixation. Fluorescence images were acquired using an ISIT (intensified silicon-intensified tube) camera, and phase images using a nuvicon camera. All images were averaged for 16 frames and recorded on optical disk. Fluorescence intensity profiles were obtained by averaging three adjacent lines of pixels.

(Fig. 3*a*), nor did the half-life vary with position in the tail (Fig. 3*b*). Thus turnover rate and, by implication, individual filament depolymerization rate, are constant throughout the tail. Electron microscopy of fixed infected cells has shown that the actin filaments in the tail average ~0.2 μm in length[2,3]. A filament of 0.2 μm comprises about 73 subunits[6]. The off-rate of ADP-actin monomers from the barbed end of a filament *in vitro* is ~7 s^{-1} (ref. 7), so filaments of this length could completely depolymerize in as little time as 10 s.

Rapidly moving bacteria appeared by phase microscopy to have longer tails than slowly moving ones. Quantitation of the relationship between bacterium speed and phase-dense tail length revealed a strong, positive and linear correlation (Fig. 3*c*).

Recent *in vivo*[8] and permeabilized cell[9] experiments have shown that exogenous actin monomers are preferentially incorporated into the tails near the bacterium surface. Combining our data with these reports, we arrive at a simple coherent view of the genesis and behaviour of the actin-rich tails of

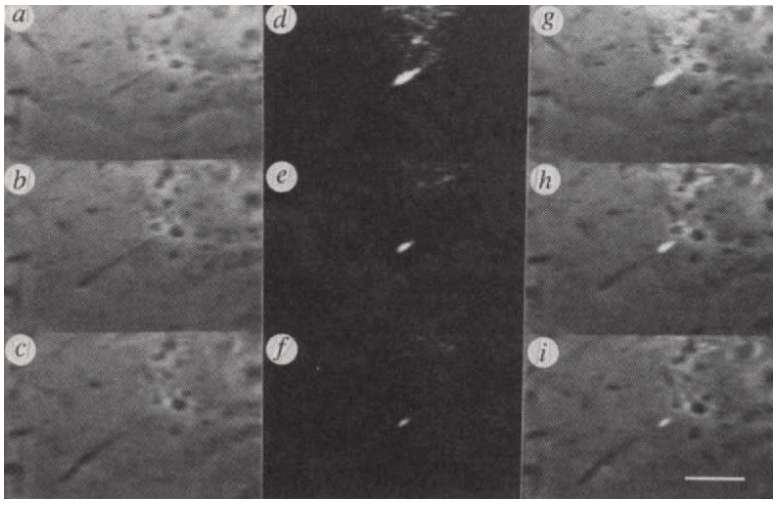

FIG. 2 Photoactivation of CR-actin in the tail of a moving bacterium. *a–c*, Phase-contrast, *d–f*, resorufin fluorescence, and *g–i*, superimposed phase and fluorescence images taken roughly 4 (*a, d, g*), 70 (*b, e, h*) and 125 (*c, f, i*) seconds after photoactivation. Scale bar, 10 μm. Note that the activated zone remains stationary in the cytoplasm, and that its intensity decreases with time.

METHODS. Infected PtK2 cells were microinjected with CR-actin as described[4]. CR-actin was allowed to incorporate for 30 min to 1 h and then a short segment of the tail was photoactivated[5] with a narrow slit of 360 nm ultraviolet light. Paired phase and fluorescence images were collected using the ISIT camera roughly 1 s apart every 11 s. The grainy appearance of the phase image is due to the poor resolution of the ISIT camera. The full length of the phase-dense tail is not visible in *a* and *b* because the bacterium is moving out from underneath the nucleus and the tail is partially obscured. The combined background fluorescence and noise level was 2–5% of the peak-activated intensity. Therefore we can state that at least 95% of the filaments in the tail behaved as a single population that remained stationary in the cytoplasm.

L. monocytogenes (Fig. 4). Short actin filaments are polymerized at the proximal end of the tail, near the bacterium surface. The newly created filaments are incorporated into a tail structure that is stationary in the cytoplasm, where they become coated and crosslinked by actin-binding proteins[1]. The rate of bacterium movement is simply equal to the rate of tail growth at the proximal end. The filaments depolymerize in a stochastic process with an average half-life of 33 s, resulting in an exponential decay of filament density in the tail both in time and in space (Fig. 1*c*).

This model makes a prediction about expected tail length. If filament nucleation and polymerization occur only at the bacterial surface, and if depolymerization is uniform and independent of speed, then the length of the tail as visible by phase should increase with the rate of bacterial movement. Recall that the phase-dense tail represents a segment of an exponential decay curve (Fig. 1*c*). Each segment of the tail, once created, persists, and is visible by phase for a certain length of time, specifically for the length of time it takes for the filament density to fall below 30–50% of the peak density. Therefore, the persistence time is expected to be 1–2 times the average filament half-life. Faster-moving bacteria are expected to have longer tails because they move further away from a newly created segment of the tail before it disappears. The slope of the line giving the relationship between tail length and bacterium speed, which we determined to be 42 s (s.d. = 10, $n = 20$; Fig. 3*c*) is a direct measurement of this persistence time. The average filament half-life measured by fluorescence decay (33 s) agrees with this value. The agreement of these values has two implications. First, it confirms the dynamic model and the conclusion that filaments in the tail are formed only at the bacterium surface[8,9]. Second, it provides independent confirmation that the photoactivation technique is giving us reliable values for actin filament turnover rates.

The *L. monocytogenes* tail is now the best understood example of a dynamic actin filament assembly, but among the questions that remain are how these filaments are nucleated, how the force for motility is generated, and what is applicable to actin filament organization and cell locomotion in general.

The nucleation mechanism involves formation of filaments without a preferred orientation[2,3], which are either released after nucleation or maybe are never directly attached to the bacterium at all. To explain these observations, we propose that the bacterium does not act as a template for filament nucleation[10], but rather by locally activating G-actin into a form that spontaneously nucleates and polymerizes into filaments. One bacterial surface protein implicated in this process is the *actA* gene product[11]. As we do not yet know what prevents cytoplasmic G-actin from polymerizing spontaneously, the activation mechanism is unclear. Current thinking implicates both exchange of ATP for ADP and removal of small, monomer-sequestering proteins in this process.

The mechanism by which the dynamic filament assembly of the tail generates protrusive force remains to be identified. Our data are consistent with the hypothesis that *L. monocytogenes* propulsion is driven solely by actin polymerization[12], effectively using the polymerization-competent G-actin pool as the power source. Replenishing this pool must in some way depend on ATP hydrolysis by actin during polymerization. One way that filament nucleation and elongation may be transduced into force generation is by rectifying or ratcheting the brownian motion of the bacterium or of the filaments (G. Oster, personal communication). It is also possible that ATPase motor proteins that are attached to the bacterium play some part in movement. Membrane-dependent osmotic forces, which may be responsible for lamellipodial extension[13], are presumably not involved in *L. monocytogenes* propulsion as the bacteria move rapidly in the bulk cytoplasm of the host cell without close association with the plasma membrane.

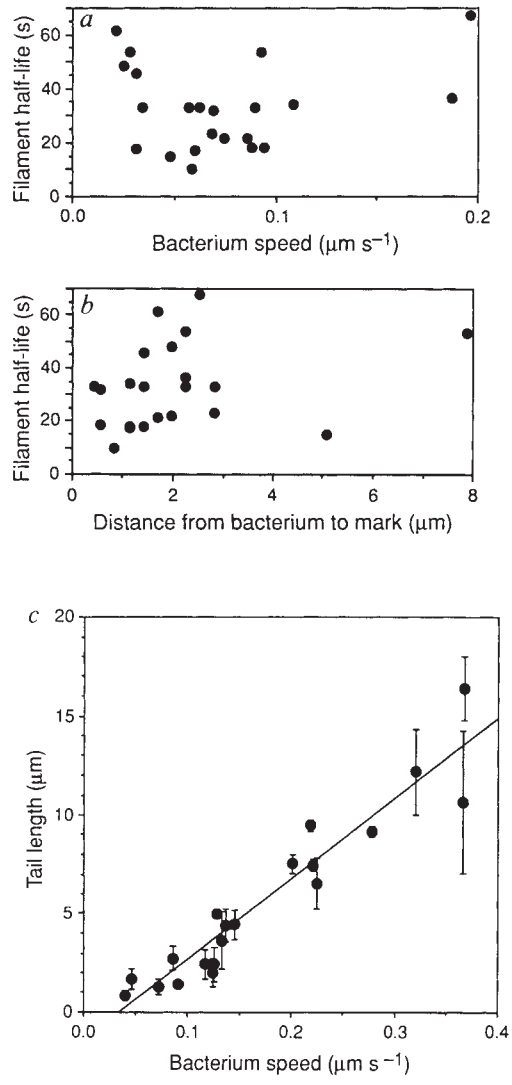

FIG. 3 Correlations among filament half-life, position in tail, bacterium speed, and length of tail. *a*, Plot of filament half-life as a function of bacterium speed. *b*, Plot of filament half-life as a function of position in the tail, defined as distance from bacterium to photoactivated mark. Each point in *a* and *b* represents an individual photoactivated tail. Both *a* and *b* are interpreted as showing no correlation. *c*, Correlation between bacterium speed and tail length. Line shown is best fit.

METHODS. Photoactivated tails of 22 bacteria moving in injected cells are represented in both *a* and *b*. Twenty other individual bacteria, observed by phase-contrast in uninjected cells, are represented in *c*. For *a* and *b*, filament half-lives were measured by fitting an exponential decay curve to a plot of total fluorescence intensity versus time for each activated tail. Illumination conditions were chosen so that photobleaching accounted for <5% of total fluorescence decay. Bacterium speeds were averaged over 55 s by fitting a straight line to a plot of distance moved versus time, with positions measured every 11 s. Distance from bacterium to mark was defined as the distance from the back end of the bacterium to the middle (peak) of the activated mark, immediately after activation. In *c*, for each bacterium, speed was averaged over 1 min by fitting a straight line to a plot of distance moved versus time, with positions measured every 10 s. For all individuals shown, the speed remained roughly constant over the period of observation ($R^2 > 0.96$ for every fitted line). Tail length was measured at the beginning, middle and end of this period (at 0, 30 and 60 s). Error bars show standard deviations of the three tail-length measurements. The tails did not tend to grow or shrink over time for bacteria moving at constant speeds; the error bars reflect uncertainty in assigning the position of the distal end of the tail. Tail length was measured from the apparent back end of the bacterium as seen by phase; the tendency of the camera to exaggerate the size of very phase-dense objects and the fact that the filaments of the tail also coat the back half of the bacterium[2,3] result in a consistent slight underestimation of true tail length.

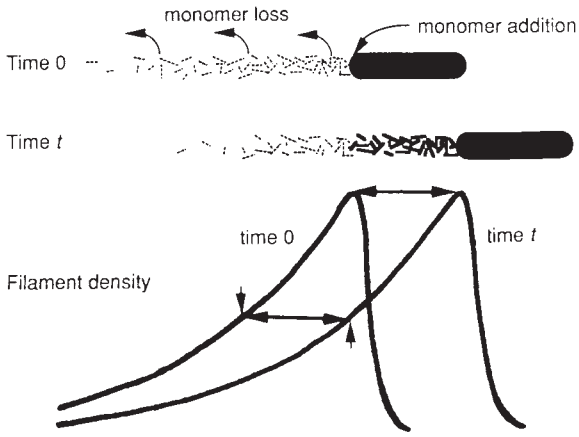

FIG. 4 Diagram of actin filament dynamics in *L. monocytogenes* tails. Actin filaments in the tail (dotted lines) remain stationary in the cytoplasm as the bacterium moves forward. New actin filaments are polymerized at the front end of the tail (heavy lines) at the same rate as the bacterium moves. Depolymerization (monomer loss) occurs at a constant rapid rate throughout the tail. This results in a distribution of actin filament density which approximates exponential decay in both space and time. As the bacterium moves forward, the filament density at each point in the tail decreases a constant percentage per unit time (exponential decay), so in the steady state the shape of the tail is maintained as an exponential curve of filament density which has been shifted in space. The arrowheads indicate the approximate position at which the tail is no longer visible in phase. The double arrrow indicates the distance the bacterium has moved; note that the end of the bacterium and the apparent end of the tail as visible in phase have moved the same distance. The result is a tail that appears by phase microscopy to remain constant in length as the bacterium moves. The length of the tail is proportional to the speed of bacterium movement as faster-moving bacteria travel a greater distance from each newly created segment of the tail before the segment decays to background phase density.

The dynamic behaviour of actin filaments in *L. monocytogenes* tails is in many ways similar to the behaviour of filaments in the lamellipodia of motile keratocytes[4] and fibroblasts (J.A.T. and T.J.M., manuscript submitted). In each case, short actin filaments are formed preferentially at the front of the actin-rich structure. Filaments are released after nucleation and cross-linked into a loosely ordered meshwork; once in the network their turnover rate is high. Turnover releases G-actin, which can then diffuse to the front of the array and polymerize again. The role of the lamellipodial networks, like the *L. monocytogenes* tail, is to generate protrusive force at the front of the array. The use of *L. monocytogenes* as a model system for studying actin-based cell motility offers the possibilities of genetic manipulation and reconstitution of motility in the absence of membranes, thereby increasing our understanding of this universal propulsive mechanism. □

Received 13 January; accepted 3 April 1992.

1. Dabiri, G. A., Sanger, J. M., Portnoy, D. A. & Southwick, F. S. *Proc. natn. Acad. Sci. U.S.A.* **87,** 6068–6072 (1990).
2. Tilney, L. G. & Portnoy, D. A. *J. Cell. Biol.* **109,** 1597–1608 (1989).
3. Tilney, L. G., Connelly, P. S. & Portnoy, D. A. *J. Cell Biol.* **111,** 2979–2988 (1990).
4. Theriot, J. A. & Mitchison, T. J. *Nature* **352,** 126–131 (1991).
5. Mitchison, T. J. *J. Cell Biol.* **109,** 637–652 (1989).
6. Egelman, E. H., Francis, N. & DeRosier, D. D. *Nature* **298,** 131–135 (1982).
7. Pollard, T. D. *J. Cell Biol.* **103,** 2747–2754 (1986).
8. Sanger, J. M., Mittal, B., Southwick, F. S. & Sanger, J. W. *J. Cell Biol.* **111,** 415a (1990).
9. Tilney, L. G., DeRosier, D. J., Weber, A. & Tilney, M. S. *J. Cell Biol.* (in the press).
10. Sanders, M. S. & Wang, Y.-L. *J. Cell Biol.* **110,** 359–365 (1990).
11. Kocks, C. *et al. Cell* **68,** 521–531 (1992).
12. Hill, T. L. & Kirschner, M. W. *Proc. natn. Acad. Sci. U.S.A.* **79,** 490–494 (1982).
13. Oster, G. F. & Perelson, A. S. *J. Cell Sci. Suppl.* **8,** 35–54 (1988).

ACKNOWLEDGEMENTS. This work was funded by fellowships from the Packard and Searle Foundations to T.J.M. J.A.T. is a Howard Hughes Medical Institute Predoctoral Fellow. Additional support was provided by the Markey Foundation through the UCSF microscopy facility.